

**Cite this article as:** Yang Xia, He Dongsheng, Du Xiaozhong, et al. Microstructure and Mechanical Properties of 6061 Al/AZ31B Mg/6061 Al Symmetrical Laminated Plate[J]. Rare Metal Materials and Engineering, 2021, 50 (04):1223-1232.

# Microstructure and Mechanical Properties of 6061 Al/AZ31B Mg/6061 Al Symmetrical Laminated Plate

Yang Xia<sup>1</sup>, He Dongsheng<sup>1,2</sup>, Du Xiaozhong<sup>1</sup>, Wang Rongjun<sup>1</sup>

<sup>1</sup> College of Mechanical Engineering, Taiyuan University of Science and Technology, Taiyuan 030024, China; <sup>2</sup> Jinxi Industries Group Co., Ltd, Taiyuan 030024, China

**Abstract:** Based on theoretical and simulation analysis, the 6061 Al/AZ31B Mg/6061 Al laminated plates were fabricated by hot rolling, and the microstructure and mechanical properties were investigated. The best coverage rate of 6061 Al of the laminated plate was obtained by classical laminated plate theory and the optimal reduction rate of the laminated plate was obtained by finite element method (FEM). According to the theoretical and simulation results, the rolling experiments of 6061 Al/AZ31B Mg/6061 Al laminated plate were carried out under different rolling temperatures, reduction rates and annealing time. And the microstructure experiment, tensile property test and energy spectrum analysis of the laminated plates were carried out. The results show that refined grains are discovered in the Mg layer at the interface, and the formation of an intermetallic compound layer consisting of  $Mg_{17}Al_{12}$  and  $Mg_2Al_3$  is identified at the interface. For the mechanical properties, with the increase of rolling reduction rate, the tensile strength, elongation and interface diffusion thickness of the 6061 Al/AZ31B Mg/6061 Al laminated plate increase significantly; with the increase of rolling temperature, the tensile strength, elongation and interface diffusion thickness of the laminated plate decrease greatly; with the increase of annealing time, the tensile strength decreases and interface diffusion thickness of the laminated plate increases.

**Key words:** multilayer composite; interfacial bonding strength; evolution of interlaminar organization; thickness of bonding layer

Magnesium alloy is the lightest metal structure material at present, and because of its low density, high specific strength, good electromagnetic shielding performance and excellent vibration reducing performance, magnesium alloys are widely used in transportation, electronic industrial products, aerospace and other fields<sup>[1-3]</sup>. However, the application of magnesium alloy is hindered by its corrosion resistance and poor deformation ability. Aluminum alloys have the advantages of good corrosion resistance, high plasticity, low production cost, convenient recovery and reuse<sup>[4-6]</sup>. Cladding Al layer on the surface of Mg alloys can greatly improve the corrosion resistance of Mg alloys<sup>[7,8]</sup>. Al-Mg-Al laminated plates take into account the excellent characteristics of the two metals; it can make up for their shortcomings and expand their application range.

Rolling lamination is the plastic deformation of two or more

kinds of metal plates through the pressure of rolling mill, which makes the hardened layer of surface metal break, and the internal metal is extruded from the crack and contacts with each other to form a solid bonding point. This processing method has the advantages of easy operation, low cost, stable performance, etc<sup>[9,10]</sup>. For magnesium alloys, because of their hexagonal crystal structure and poor plastic processing at room temperature, Al-Mg-Al laminated plates are often prepared by hot rolling<sup>[11,12]</sup>.

In recent years, scholars have conducted a lot of research on Mg-Al laminated plates by rolling. Zhang et al<sup>[13]</sup> prepared 7075 Al/AZ31B Mg/7075 Al laminated composites by hot rolling bonding method and evaluated microstructure and bonding strength of the experimental laminated composites, and thickness ratio of the constituent layers after hot rolling. Liu et al<sup>[14]</sup> prepared two types of laminated metal composites (LMCs, i. e., Mg/Mg and Mg/Al/Mg)

Received date: September 25, 2020

Foundation item: National Natural Science Foundation of China (51504157); China Postdoctoral Science Foundation (2016M601288); Shanxi Province Science and Technology Major Special Project (20181102015)

Corresponding author: Yang Xia, Ph. D., Professor, College of Mechanical Engineering, Taiyuan University of Science and Technology, Taiyuan 030024, P. R. China, Tel: 0086-351-6998115, E-mail: yangxia@tyust.edu.cn

with different reduction ratios via warm roll bonding. Microstructure investigation, tensile and three-point bending tests were conducted to test the properties of the LMCs. Luo et al<sup>[15]</sup> prepared Al/Mg/Al laminated plate by two passes of hot rolling process at different temperatures. It was found that there were no new compounds on the bonding surface after the first low temperature rolling. With the increase of annealing temperature, the growth rate of the new compound increases, and inter-metallic compounds brake in the second pass of high temperature hot rolling. Nie et al<sup>[16]</sup> fabricated Al/Mg/Al laminates by hot rolling at 400 °C and annealed at temperature ranging from 200 °C to 400 °C for 1~4 h. Microstructural examination revealed that brittle intermetallic identified as Mg<sub>17</sub>Al<sub>12</sub> and Al<sub>3</sub>Mg<sub>2</sub> appears at Mg/Al interface when annealing temperature exceeds 300 °C. Luo et al<sup>[17]</sup> fabricated 5052/AZ31B/5052 composite plates by two-pass hot rolling, under the rolling parameters of 623 K/15 min/40% for the first pass and 673 K/10 min/50% for the second pass. The structure and element change in the zone of the joint interface were studied by optical microscope (OM), scanning electron microscope (SEM), and energy dispersion spectrum (EDS). Lee et al<sup>[18]</sup> investigated the influence of annealing and secondary warm rolling on the microstructural evolution and mechanical properties of a roll-bonded three-ply Al/Mg/Al sheet. After annealing at 300 °C, the formation of an intermetallic compound (IMC) layer consisting of Mg<sub>17</sub>Al<sub>12</sub> and Mg<sub>2</sub>Al<sub>3</sub> was identified at the interface. Kim et al<sup>[19]</sup> prepared Al/Mg laminated plate by hot rolling process, and studied the effect of annealing temperature and rolling pass on the microstructure and properties of the interface of the laminated plate. Gajanan et al<sup>[20]</sup> used accumulative roll bonding (ARB) process to develop Mg-6% Zn/Al and Mg-6% Zn/anodized-Al multi-layered composites and conducted microstructural characterization by scanning electron microscopy, energy-dispersive X-ray spectroscopy, electron backscattered diffraction, and transmission electron microscopy. Wang et al<sup>[21]</sup> fabricated Ti/Al/Mg/Al/Ti laminates by hot rolling at 450 °C with various rolling reductions, and the relationship between the mechanical properties and microstructures was investigated in detail.

The laminated effect of the laminated surface is related to rolling temperature, reduction rate and annealing temperature. Therefore, before the rolling experiment, it is very important to determine the best rolling parameters by theoretical analysis. In this study, 6061 Al/AZ31B Mg/6061 Al laminated plates were fabricated by hot rolling based on theoretical and simulation analysis, and the microstructure and mechanical properties were investigated by microstructure experiment, tensile property test and energy spectrum analysis. With the results, it is of great scientific and practical significance to improve the production technology of Mg/Al laminated plates and promote the application field of laminated materials.

## 1 Theoretical Calculation and FEM Simulation of 6061 Al/AZ31B Mg/6061 Al Laminated Plate

### 1.1 Theoretical calculation of 6061 Al/AZ31B Mg/6061 Al laminated plate

Fig. 1 shows the geometric diagram of the laminated

plate. Because the stiffness and strength analyses of laminated plates are more complex than those of single-layer plates, the single-layer plates that make up laminated plates are generally regarded as thin plates with uniform properties. As the basic elements of laminated plates, their thickness is much smaller than length and width, so each single-layer plate is approximately regarded as a plane stress state<sup>[22]</sup>.

Magnesium alloys and aluminum alloys are regarded as isotropic materials.  $\sigma_1$ ,  $\sigma_2$  and  $\tau_{12}$  represent the normal stress and shear stress under the action of the external force, respectively.  $\varepsilon_1$ ,  $\varepsilon_2$  and  $\gamma_{12}$  represent the corresponding strain. According to the classical laminated plate theory, the stress-strain relationship of a single-layer plate in a plane stress state is shown in Eq.(1).

$$\begin{bmatrix} \sigma_x \\ \sigma_y \\ \tau_{xy} \end{bmatrix} = \begin{bmatrix} Q_{11} & Q_{12} & 0 \\ Q_{21} & Q_{22} & 0 \\ 0 & 0 & Q_{66} \end{bmatrix} \begin{bmatrix} \varepsilon_x \\ \varepsilon_y \\ \gamma_{xy} \end{bmatrix} = \begin{bmatrix} E & \nu E & 0 \\ 1-\nu^2 & 1-\nu^2 & 0 \\ \nu E & E & 0 \\ 1-\nu^2 & 1-\nu^2 & 0 \\ 0 & 0 & \frac{E}{2(1+\nu)} \end{bmatrix} \begin{bmatrix} \varepsilon_x \\ \varepsilon_y \\ \gamma_{xy} \end{bmatrix} \quad (1)$$

In this study, magnesium alloy AZ31B and aluminum alloy 6061 were adopted. The mechanical properties of AZ31B Mg and 6061 Al are shown in Table 1.

#### 1.1.1 Theoretical calculation of stiffness of 6061 Al/AZ31B Mg/6061 Al laminated plate

The stiffness expression of the laminated plate is shown in Eq.(2).

$$\begin{cases} A_{ij} = \sum_{k=1}^n Q_{ij}^{(k)} (z_k - z_{k-1}) \\ B_{ij} = \frac{1}{2} \sum_{k=1}^n Q_{ij}^{(k)} (z_k^2 - z_{k-1}^2) \\ D_{ij} = \frac{1}{3} \sum_{k=1}^n Q_{ij}^{(k)} (z_k^3 - z_{k-1}^3) \end{cases} \quad (2)$$

Because this study is based on the plane stress hypothesis, the coupling stiffness  $B_{ij} = 0$ . Assuming that  $N^* = N/h$ ,  $M^* = 6M/h^2$ ,  $A_{ij}^* = A_{ij}/h$ ,  $B_{ij}^* = 2B_{ij}/h^2$ ,  $D_{ij}^* = 12D_{ij}/h^3$  and the total thickness  $h$  of the 6061 Al/AZ31B Mg/6061 Al laminated

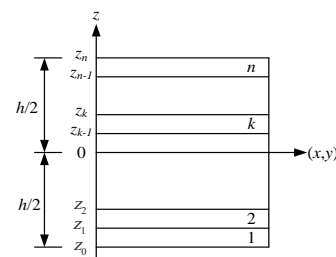


Fig.1 Geometric diagram of the laminated plate

Table 1 Mechanical properties of materials

Material	$E/\text{MPa}$	$\nu$	$\rho/\text{g}\cdot\text{cm}^{-3}$	$\sigma_s/\text{MPa}$	$\sigma_m/\text{MPa}$
6061 Al	68950	0.3	2.71	276	310
AZ31B Mg	43000	0.31	1.77	140	240

plate is 1, the thickness of single-layer 6061 Al pate is  $t$ , the thickness of AZ31B Mg layer is  $1-2t$  ( $0 \leq t \leq 0.5$ ), and coverage rate of 6061 Al is  $2t^{[23]}$ , the expression of regularized stiffness coefficient of laminated plate can be obtained, as shown in Eq. (3).

$$\begin{cases} A_{11}^* = 2t(Q_{11}^{(1)} - Q_{11}^{(2)}) + Q_{11}^{(2)} = A_{22}^* = A_{12}^* + 2A_{66}^* \\ D_{11}^* = (8t^3 - 12t^2 + 6t)(Q_{11}^{(1)} - Q_{11}^{(2)}) + Q_{11}^{(2)} \\ \quad = D_{22}^* = D_{12}^* + 2D_{66}^* \end{cases} \quad (3)$$

Substitute the corresponding parameters in Table 1 into Eq.(3), the regularized tensile and bending stiffness coefficient of 6061 Al/AZ31B Mg/6061 Al laminated plates can be obtained. The curves of the stiffness and specific stiffness (specific stiffness is obtained by dividing stiffness by density) of the 6061 Al/AZ31B Mg/6061 Al laminated plate with the coverage rate of the 6061 Al are shown in Fig.2.

It can be seen from Fig.2 that the tensile stiffness and bending stiffness of the laminated plate increase with the increase of the coverage rate of 6061 Al. And the tensile specific stiffness of the laminated plate increases slightly with the increase of the coverage rate of 6061 Al. The bending specific stiffness increases at first and then decreases with the increase of coverage rate of 6061 Al. When the coverage rate of 6061 Al is 0.4, the bending specific stiffness of the laminated plate is the maximum and the value is 32 574 MPa/(g·cm<sup>-3</sup>), which is 18.6% higher than that of AZ31B Mg and 16.5% higher than that of 6061 Al. In this situation, the specific stiffness per-

formance of the laminated plate is optimum.

### 1.1.2 Theoretical calculation of strength of 6061 Al/AZ31B Mg/6061 Al laminated plate

It is assumed that the failure strength of the first layer metal is the yield strength of the laminated plate, and  $M_x, M_y, M_{xy}$  are the internal torque (bending or torque) per unit width of the cross section of the laminated plate.  $k$  represents the  $k$ -layer of the laminated plate. The stress of the  $k$ -layer of the laminated plate can be expressed as:

$$\begin{bmatrix} \sigma_x \\ \sigma_y \\ \tau_{xy} \end{bmatrix}_k = \begin{bmatrix} Q_{11} & Q_{12} & 0 \\ Q_{21} & Q_{22} & 0 \\ 0 & 0 & Q_{66} \end{bmatrix}_k \begin{bmatrix} \varepsilon_x^0 \\ \varepsilon_y^0 \\ \gamma_{xy}^0 \end{bmatrix} + z \begin{bmatrix} \kappa_x \\ \kappa_y \\ \kappa_{xy} \end{bmatrix} \quad (4)$$

where  $\{\kappa\}$  is the curvature of bending and distorting deformation of the symmetry plane of the middle-layer metal of the laminated plate;  $\varepsilon_{ij}^0$  is the normal and shear strain on the symmetry plane of the middle-layer metal;  $[Q_{ij}]_k$  is the stiffness matrix of the  $k$ -layer plate;  $z$  is the coordinate of the thickness direction of the  $k$ -layer plate.

When the laminated plate is only subjected to internal torque,  $\{\varepsilon^0\} = 0$ , Eq.(6) can be written as

$$\begin{bmatrix} \sigma_x \\ \sigma_y \\ \tau_{xy} \end{bmatrix}_k = z^* \begin{bmatrix} Q_{11} & Q_{12} & 0 \\ Q_{21} & Q_{22} & 0 \\ 0 & 0 & Q_{66} \end{bmatrix}_k \begin{bmatrix} D_{11}^* & D_{12}^* & 0 \\ D_{21}^* & D_{22}^* & 0 \\ 0 & 0 & D_{66}^* \end{bmatrix}^{-1} \begin{bmatrix} M_x^* \\ M_y^* \\ M_{xy}^* \end{bmatrix} \quad (5)$$

It is assumed that the laminated plate only bears internal torque in the  $x$  direction, and it is only necessary to check the  $x$ -direction strength of each single-layer.

$$\begin{cases} \sigma_x^{(k)} = z^* \frac{D_{11}^* Q_{11}^{(k)} - D_{12}^* Q_{12}^{(k)}}{A_{11}^{*2} - A_{12}^{*2}} M_x^* \\ \sigma_y^{(k)} = z^* \frac{D_{11}^* Q_{12}^{(k)} - D_{12}^* Q_{11}^{(k)}}{D_{11}^{*2} - D_{12}^{*2}} M_x^* \\ \tau_{xy}^{(k)} = 0 \end{cases} \quad (6)$$

Assuming that the regularized internal torque  $M_x^*$  is equal to the yield strength of Mg alloy, the relevant data is substituted into the above formula.

$$\begin{cases} \sigma_x^{(1)} = \frac{15.3s + 3.3}{44.7s^2 + 19.5s + 2.09} M_x^* \\ \sigma_x^{(2)} = \frac{(9.74s + 2.09) \times (1 - 2t)}{44.7s^2 + 19.5s + 2.09} M_x^* \end{cases} \quad (7)$$

The failure strength formula of the 6061 Al/AZ31B Mg/6061 Al laminated plate can be obtained as follows:

$$\sigma_s' = \frac{44.7s^2 + 19.5s + 2.09}{(9.74s + 2.09) \times (1 - 2t)} R_c^{(2)} \quad (0 < t < 0.1) \quad (8)$$

$$\sigma_s' = \frac{44.7s^2 + 19.5s + 2.09}{15.3s + 3.3} R_c^{(1)} \quad (0.1 \leq t < 0.5) \quad (9)$$

The relation of failure strength and specific strength of the laminated plate with coverage rate of Al alloy is shown in Fig.3.

It can be seen from Fig.3a that with the increase of coverage rate of Al alloy, the tensile and bending strengths

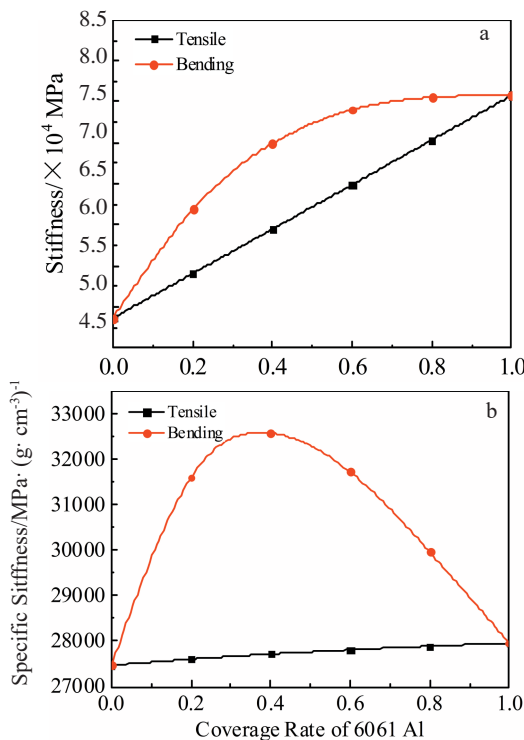


Fig.2 Curves of stiffness (a) and specific stiffness (b) of the laminated plate

of the laminated plate increase, and the bending strength is always higher than that of the tensile strength. It can be seen from Fig. 3b that the tensile specific strength of the 6061 Al/AZ31B Mg/6061 Al laminated plate changes little. With the increase of coverage rate of Al alloy, the bending specific strength of laminated plate increases first and then decreases. When the coverage rate of Al alloy is 0.4, the bending specific strength of laminated plate reaches the maximum value of  $118.7 \text{ MPa}/(\text{g} \cdot \text{cm}^{-3})$ , which is 50% higher than that of Mg alloy, and 16% higher than that of Al alloy. The optimum thickness ratio of the 6061 Al/AZ31B Mg/6061 Al laminated plate is 1:3:1.

## 1.2 Analysis of FEM simulation results

Adopting the optimum thickness ratio, the 6061 Al alloy plate with one layer thickness of 1 mm and the AZ31B Mg alloy plate with 3 mm in thickness were selected to simulate the hot rolling process of the Al/Mg/Al symmetrical laminated plate by FEM software-Deform. Through the hot rolling process simulation, we can obtain parameters such as temperature field, stress field, strain field and rolling force of the laminated plate. However, only vertical compressive stress and equivalent strain are useful for determining whether the laminated plate is effectively combined.

### 1.2.1 Vertical compressive stress of the laminated plates

Vertical compressive stress is an important factor in determining whether the laminated plate is in plastic deformation state [24].

According to the hot working characteristics of Al alloys and Mg alloys,  $400 \text{ }^\circ\text{C}$  was selected as the rolling temperature [25]. When roll angular velocity is  $0.5 \text{ rad/s}$ , rolling temperature is  $400 \text{ }^\circ\text{C}$  and reduction rates are 25%, 30%, 35% and 40%, the variation of vertical compressive stress of laminated plates under different reduction rates along rolling deformation zone length is shown in Fig.4.

It can be seen from Fig.4 that with the increase of reduction rate, the maximum vertical compressive stress near the interface increases. When the reduction rate is 25% and rolling temperature is  $400 \text{ }^\circ\text{C}$ , the average value of the maximum vertical compressive stress near the interface is about  $74.8 \text{ MPa}$ . It is slightly greater than the deformation resistance of 6061 Al, which is  $71.4 \text{ MPa}$ , indicating that the interface of the laminated plate can meet the bonding conditions in this situation. Considering material damage characteristics, the optimum relative reduction rate should be more than 25%.

### 1.2.2 Equivalent strain of laminated plates

The equivalent strain contour of the laminated plate in the length direction of the rolling deformation area is shown in Fig.5. Fig.5a and 5b show the equivalent strain of Al alloy and Mg alloy at the same point on the joint interface, when roll angular velocity is  $0.5 \text{ rad/s}$ , rolling temperature is  $400 \text{ }^\circ\text{C}$  and reduction rates are 25%, 30%, 35% and 40%. Table 2 shows the equivalent strain of the two metals.

As can be seen from Fig.5 and Table 2, with the increase of the reduction rate, the equivalent strain difference between

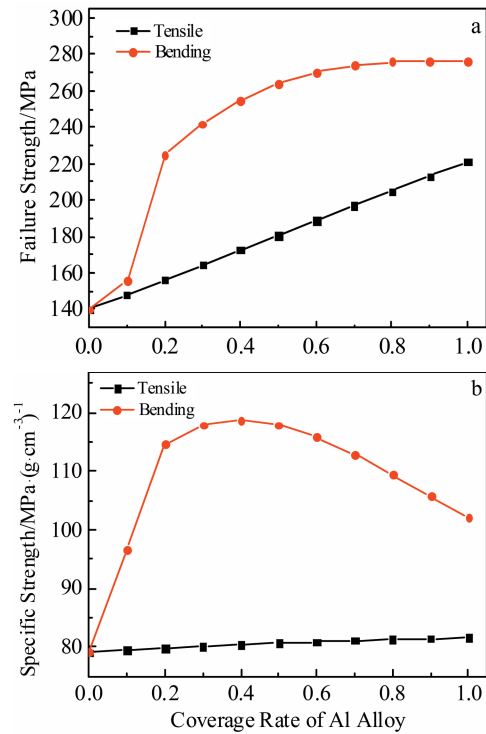


Fig.3 Failure strength (a) and specific strength (b) of the laminated plate

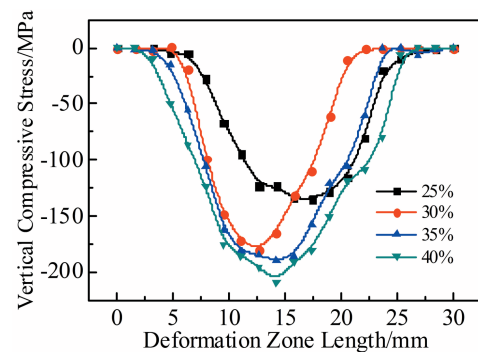


Fig.4 Vertical compressive stresses under different reduction rates

the two alloys decreases.

According to Ref. [26], when the equivalent strain value near the joint interface is less than 0.01, it can be considered that the interface is effectively combined. As can be seen above, when the reduction rate is greater than 30%, the equivalent strain difference value near the joint interface is less than 0.01, meeting the effective bonding conditions of the laminated plate.

In a word, according to the above simulation results and edge crack phenomenon of Mg alloy, it can be obtained that in order to achieve a good combination of 6061 Al/AZ31B Mg/6061 Al laminated plate, the optimal reduction rate should be more than 25%.

**Table 2** Equivalent strain of 6061 Al and AZ31B Mg

Reduction rate/%	6061 Al	AZ31B Mg	Difference
25	0.347	0.328	0.019
30	0.483	0.473	0.01
35	0.516	0.508	0.008
40%	0.630	0.624	0.005

**Table 3** Main components of AZ31B Mg alloy (wt%)

Al	Mn	Zn	Fe	Cu	Si	Ni
3.00	0.60	1.00	0.003	0.01	0.08	0.001

**Table 4** Main components of 6061 Al alloy (wt%)

Si	Fe	Cu	Mn	Mg	Cr	Zn	Ti
0.4~0.8	<0.7	0.15~0.4	<0.15	0.8~1.2	0.04~0.35	<0.25	<0.15

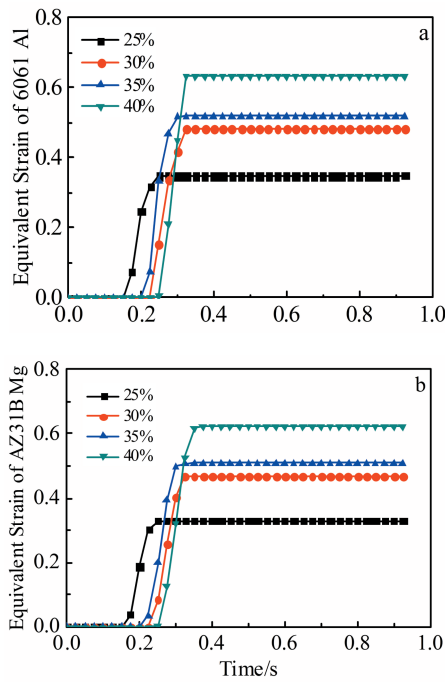


Fig.5 Equivalent strain of the laminated plate at different reduction rates: (a) Al alloy and (b) Mg alloy

## 2 Experiment

### 2.1 Material and processing

Consistent with the theoretical calculation, 6061 Al alloy and AZ31B Mg alloy were selected as component plates. The main components of the experimental materials are shown in Table 3 and Table 4. The initial dimension of the AZ31B Mg plates was 200 mm×100 mm×3 mm and 6061 Al plates were 200 mm×100 mm×1 mm. In this situation, the coverage rate of Al alloy was 0.4.

The rolling experiments of the 6061 Al/AZ31B Mg/6061 Al laminated plate were carried out on the two-roll experimental rolling mill; the rolling process is illustrated in Fig.6. The method includes the following steps: firstly, surface treatment on the laminated surface of the metal plate; secondly, riveting the three-layer metal plate, followed by heating and rolling for laminated plate according to the rolling schedule; finally, heat treatment on the laminated plate. Fig.7 shows the laminated plates before and after rolling, and the experimental results are in good agreement with the simulation analysis by FEM.

The main parameters of the rolling mill is as follows: roller size is  $\Phi 320$  mm×350 mm, motor capacity is 90 kW, motor speed is 1500~2000 r/min, the max rolling force is 1500 kN, and the max rolling speed is 2 m/s. According to the simulation results, the rolling experimental scheme of the 6061 Al/AZ31B Mg/6061 Al laminated plate specimen (S1-S7) are shown in Table 5, and the annealing temperature is 200 °C.

### 2.2 Characterization

Microstructure of the Mg layer was examined by scanning electron microscopy (SEM) and optical microscopy. Chemical component of the bond interface was characterized by scanning electron microscopy (SEM) and energy-dispersive X-ray spectroscopy (EDS). The mechanical properties were examined by the WDW-200E universal testing machine.

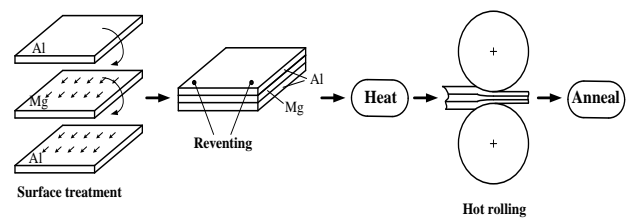


Fig.6 Specific process of hot rolling

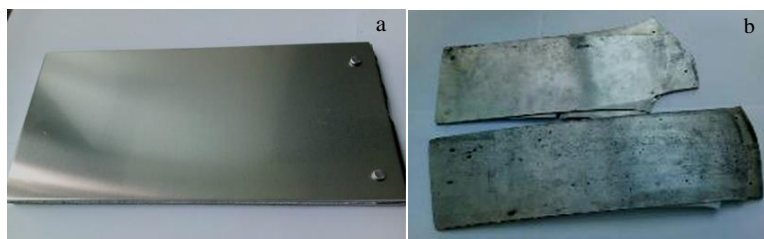


Fig.7 Laminated plate before (a) and after (b) rolling

**Table 5 Rolling experimental scheme of the laminated plate**

Specimen	S1	S2	S3	S4	S5	S6	S7
Rolling temperature/°C	400	400	400	450	400	400	400
Reduction rate/%	25	30	35	35	35	35	35
Annealing time/h	-	-	-	-	0.5	1	1.5

### 3 Results and Discussion

#### 3.1 Microstructure and composition

##### 3.1.1 Microstructure

Because there is only few slip systems in Mg alloy, the deformation is twin in the rolling process, and the microstructure of the rolled AZ31B Mg is very uneven. A large number of fine grains are produced around the elongated rolling structure, which is caused by the dynamic recrystallization of AZ31B Mg structure. Due to the rapid reduction of temperature caused by air-cooling after rolling, the recrystallized grains cannot grow, so the shape is small. Different degrees of dynamic recrystallization occur in the AZ31B Mg layer under different reduction rates. Dynamic recrystallization occurs in the experimental alloys during the hot rolling tests, and the alloy plates in the experimental composite have equiaxed grains, as shown in Fig.8.

It can be seen from Fig.8a that there are obvious original coarse grains in the AZ31B Mg layer, and the dynamic recrystallization degree is very small. A small part of recrystallized grains are produced near the grain boundary, and the grain size is refined to a certain extent, presenting a large structural heterogeneity. The original grains of AZ31B Mg are deformed, and the coarse grains are elongated along the rolling direction, so there are more larger elongated strip grains in Fig.8b. In Fig.8c, the degree of dynamic recrystallization increases, more and more recrystallized grains appear around the elongated grains, and grow continuously. With the increase of plastic deformation, the shear strain at the joint interface of AZ31B Mg and 6061 Al decreases, leading to the decrease of

the degree of structural heterogeneity. Compared with Fig.8b and 8d, the grain size of AZ31B Mg increases with the increase of rolling temperature. As shown in Fig.8e~8g, with the increase of annealing time, the recrystallized grains of AZ31B Mg grow up, the grain boundary becomes clearer, and the average grain size in Fig.8g is about 20  $\mu\text{m}$ . A large number of original grains are replaced by equiaxed grains, and the grain size is gradually unified. After annealing, there are three processes in the 6061 Al/AZ31B Mg/6061 Al laminated plate: recovery, recrystallization and grain growth. These three processes overlap and alternate, and there is no standard boundary between them.

Fig.9 shows the morphologies of the 6061 Al/AZ31B Mg/6061 Al laminated plate. It can be seen that all laminated plates have good bonding performance, and there is no obvious defects in the bonding interface. With the increase of rolling reduction rate, the bonding interface is wavy, and there is a diffusion of Al alloy and Mg alloy at the bonding interface. The observation results for the interfacial microstructure in the composite are similar to the above results, as shown in Fig.9.

##### 3.1.2 Element distribution

In order to further understand the influence of rolling reduction rate, rolling temperature and annealing time on the diffusion of two metals at the interface of 6061 Al/AZ31B Mg/6061 Al laminated plate, EDS line scanning was performed on both sides of the laminated interface by EDS spectrometer. The results are shown in Fig.10. A diffusion layer exists at the interface. In the diffusion layer, the concentration of the element Al decreases from the 6061 Al alloy side to the AZ31B Mg alloy side while the concentration distribution of the element Mg is the opposite.

Because with the increase of plastic deformation, the deformation heat of the interface between Al alloy plate and Mg alloy plate also increases, which leads to an increase in the element diffusion range; the higher the rolling temperature, the faster the metal atoms move, the larger the range of atom migration caused by thermal diffusion and the greater the thickness of diffusion layer. From Fig.10a~10d, with the increase

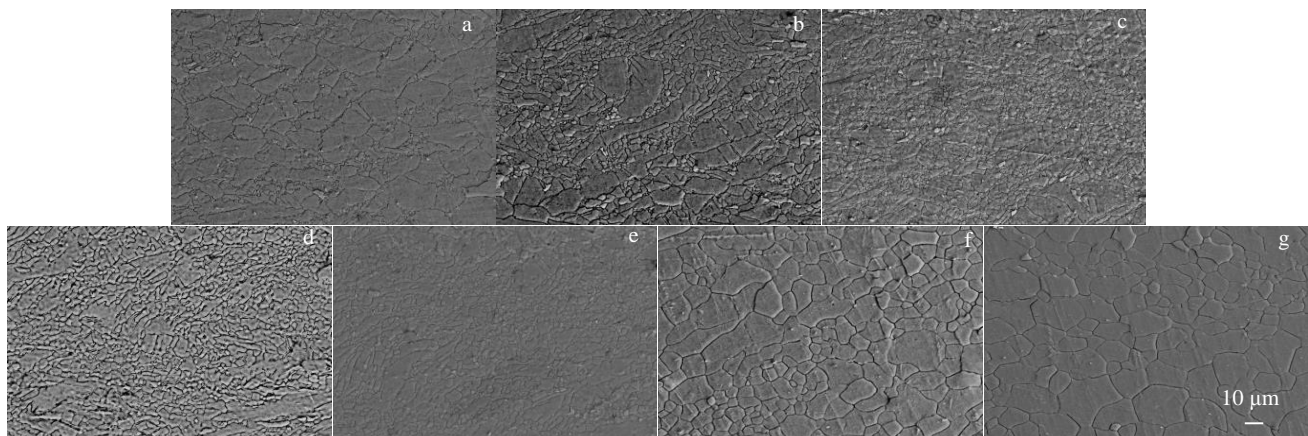


Fig.8 Microstructures of AZ31B Mg alloy at different reduction rates and temperatures: (a) 400 °C, 25%; (b) 400 °C, 30%; (c) 400 °C, 35%; (d) 450 °C, 30%; (e) 400 °C, 35%+200 °C/0.5 h; (f) 400 °C, 35%+200 °C/1 h; (g) 400 °C, 35%+200 °C/1.5 h

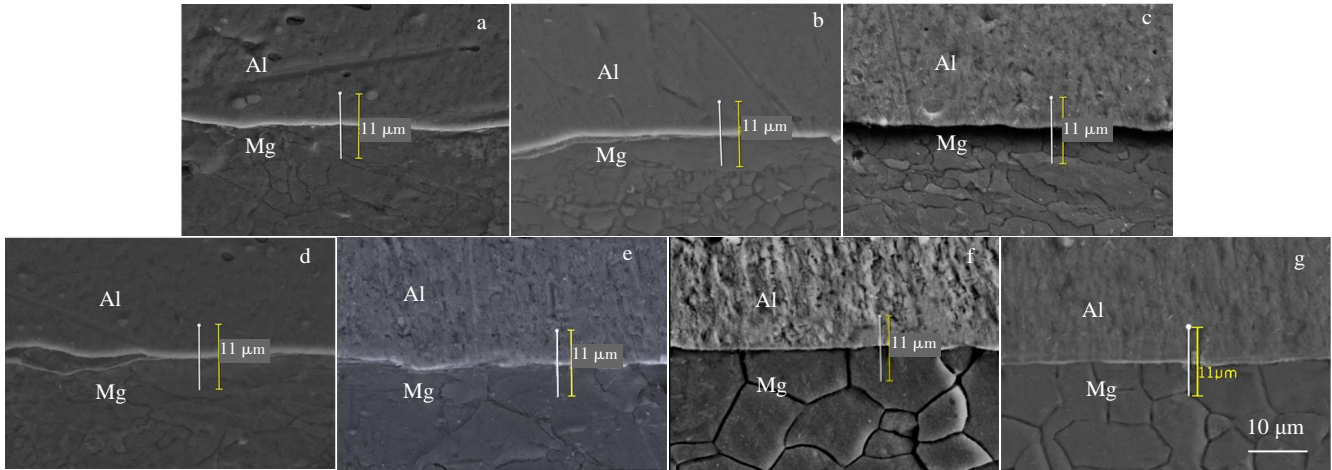


Fig.9 Representative interfacial microstructures of 6061 Al/AZ31B Mg/6061 Al laminated plates: (a) 400 °C , 25%; (b) 400 °C , 30%; (c) 400 °C , 35%; (d) 450 °C , 30%; (e) 400 °C , 35%+200 °C/0.5 h; (f) 400 °C , 35%+200 °C/1 h; (g) 400 °C , 35%+200 °C/1.5 h

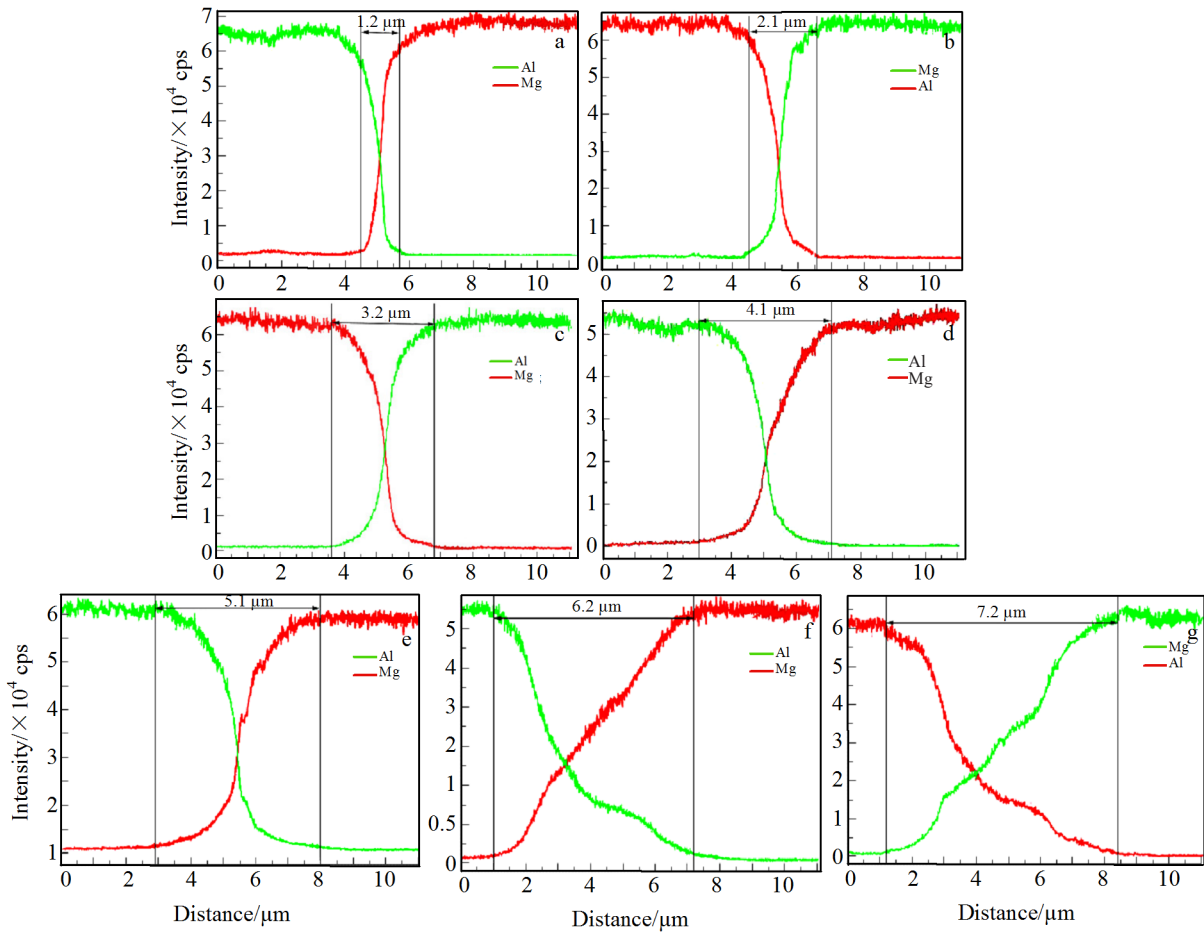


Fig.10 Elemental distributions across the Mg/Al interface of the laminated plate: (a) 400 °C , 25%; (b) 400 °C , 30%; (c) 400 °C , 35%; (d) 450 °C , 30%; (e) 400 °C , 35%+200 °C/0.5 h; (f) 400 °C , 35%+200 °C/1 h; (g) 400 °C , 35%+200 °C/1.5 h

of reduction rate and rolling temperature, the element diffusion range of Al-Mg laminated interface increases, and the diffusion layer width ranges from 1 μm to 4 μm. From Fig.10e~10g, it can be concluded that the diffusion thickness of the interlayer increases with the increase of annealing time, and the diffusion layer width ranges from 5.1 μm to 7.2 μm.

Point scanning was carried out on the bonding area of the

6061 Al/AZ31B Mg/6061 Al laminated plate. Fig. 11 shows EDS point scanning results, when the annealing time was 1 h (specimen S6). As can be seen from Fig. 11c, the proportion of Mg element to Al element is basically 2:2.94, which can be determined as the  $Mg_2Al_3$ . In Fig. 11d, the proportion of Mg element to Al element is about 1.44, which is close to that of  $Mg_{17}Al_{12}$ , so it can be basically determined that the compound is  $Mg_{17}Al_{12}$ . It

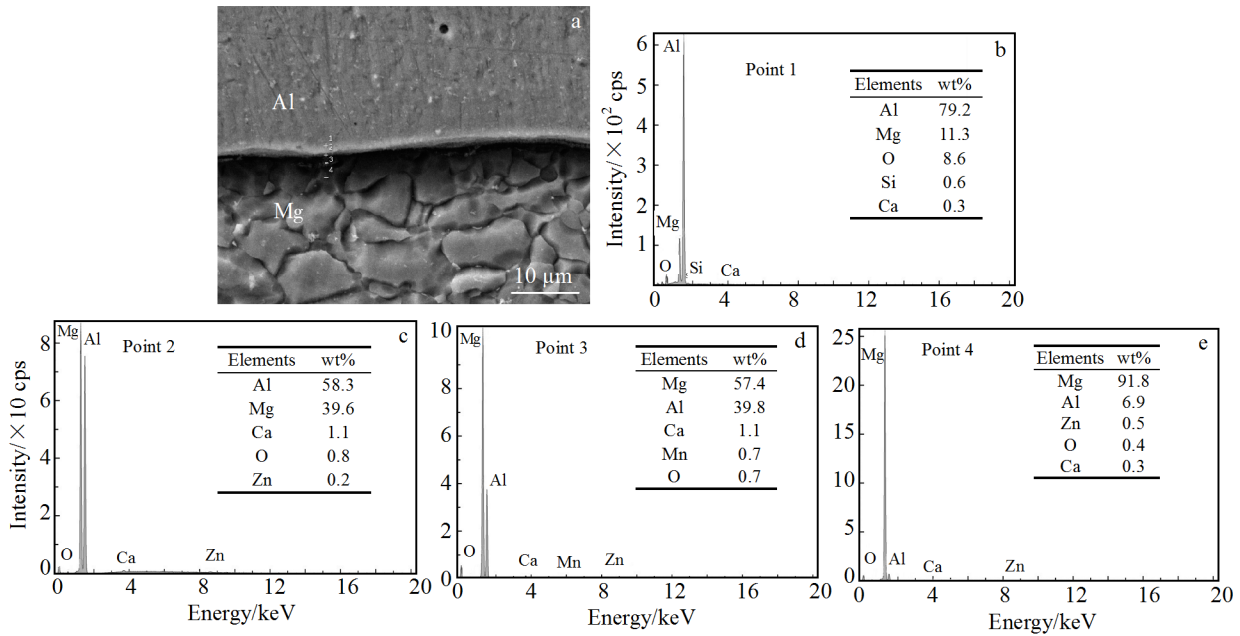


Fig.11 Specimen S6 interface (a) and EDS point scanning results on the Mg/Al interface (b~e) of the laminated plate

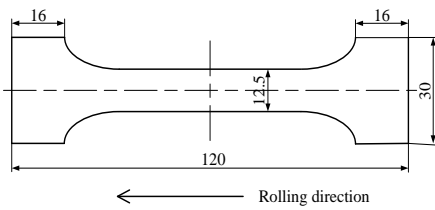


Fig.12 Schematic view of the specimen for tensile strength test

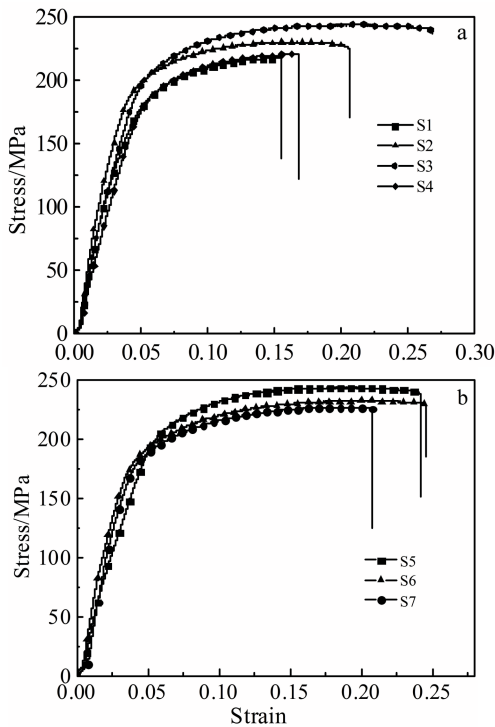


Fig.13 Stress-strain curves of specimens at different reduction rates and temperatures (a) and at different annealing time (b)

can be seen that the atomic percentage of Mg atom near the AZ31B Mg region is higher than near the 6061 Al region, indicating that  $Mg_{17}Al_{12}$  is produced near the AZ31B Mg region and  $Mg_2Al_3$  is produced near the 6061 Al region.

### 3.2 Tensile property

The WDW-200E universal testing machine was used to carry out the mechanical properties test, and the tensile speed was 0.5 mm/min. Fig. 12 shows the schematic view of the specimens for tensile strength test. Fig. 13 shows the stress-strain curves of the specimens, and Table 6 shows the results.

Therefore, it can be seen that the tensile strength, yield strength and the elongation of the 6061 Al/AZ31B Mg/6061 Al laminated plate increases with the increase of reduction rate, and decreases with the increase of the rolling temperature. In the tensile process, the tensile curve of the laminated plate only has a stress drop phenomenon, indicating that when the reduction rate is more than 25%, the Al-layer and the Mg-layer are simultaneously broken. Therefore, combined performance of the laminated plate is already very good.

As shown in Table 6, under temperature of 400 °C and

Table 6 Tensile strength and elongation of the laminated plates

Specimen	Condition	Strength/MPa	Elongation/%
S1	400 °C, 25%	210.2	17.1
S2	400 °C, 30%	225.1	20.6
S3	400 °C, 35%	243.2	23.8
S4	450 °C, 30%	217.6	15.6
S5	400 °C, 35%+200 °C/0.5 h	243.4	24.2
S6	400 °C, 35%+200 °C/1 h	232.2	24.6
S7	400 °C, 35%+200 °C/1.5 h	226.5	20.8



rolling reduction rate of 35%, the tensile strength and elongation of specimen S3 increase to 243.2 MPa and 23.8%, respectively. With the prolongation of annealing time, the tensile strength and yield strength of the laminated plate decrease gradually. Under 400 °C, 35%+200/1h condition, the tensile strength and the elongation of specimen S6 decrease to 232.2 MPa and 24.6%, respectively, which is mainly caused by the increase of grain size of Mg alloy matrix. When the annealing time is 1.5 h, the elongation of the specimen decreases significantly, only 20.8%. This is because with the increase of annealing time, due to the diffusion of alloying elements and the partial polymerization of solute atoms, the thickness of Mg-Al interlaminar compound increases, and the precipitated phase in the alloy increases, resulting in a reduction in the plasticity of the laminated plate. At the same time, due to the decrease of elongation, the hardening effect of Al alloy has not been fully played, which make the tensile strength slightly reduce.

#### 4 Conclusions

1) The classical laminated plate theory can be used to calculate the mechanical properties of the 6061 Al/AZ31B Mg/6061 Al laminated plate. When the coverage rate of Al alloy is 0.4, the thickness ratio and the mechanical properties of the laminated plate are the optimum.

2) In the FEM simulation, equivalent strain and vertical compressive stress are used to determine the combination. In order to achieve a good combination of the 6061 Al/AZ31B Mg/6061 Al laminated plate, according to the simulation results, the optimal reduction rate should be more than 25%.

3) According to the microstructure experiment and point scan results, refined grains are discovered in the Mg layer at the interface, and the formation of an intermetallic compound layer consisting of  $Mg_{17}Al_{12}$  and  $Mg_2Al_3$  is identified at the interface. With the increase of annealing time, the grain size of Mg alloy increases gradually and finally reaches 20  $\mu\text{m}$ , and then the grain size tends to be stable.

4) According to the tensile property test and energy spectrum analysis results, when the rolling temperature is 400 °C, the rolling reduction rate is 35%, the tensile strength and elongation of the 6061 Al/AZ31B Mg/6061 Al laminated plate gradually increase to 243.2 MPa and 23.8%, respectively, and the interface diffusion thickness increases to 3.2  $\mu\text{m}$ . Under 400 °C, 35%+200 °C/1 h, the tensile strength and elongation of the laminated plate decrease to 232.2 MPa and 24.6%, respectively. When the annealing time is 1.5 h, the tensile strength continues to decrease, the elongation decreases to 20.8%, and the interface diffusion thickness increases to 7.2 mm.

#### References

- Zhang Peiwu, Xia Wei, Liu Ying et al. *Materials Review*[J], 2005, 19(7): 82 (in Chinese)
- Pan Shuai, Li Qiang, Yu Baoyi, Zheng Li et al. *Rare Metal Materials and Engineering*[J], 2019, 48(7): 2379 (in Chinese)
- Zhou Lei, Zheng JingXu, Wang Xiaodong et al. *Journal of Materials Research*[J], 2020, 35(2):172
- Weatherly G C, Perovic A, Mukhopadhyay N K et al. *Metallurgical and Materials Transactions A*[J], 2001, 32(2): 213
- Zang Jie, Yu Sirong, Zhu Guang et al. *Surface and Coatings Technology*[J], 2019, 380: 125 078
- Wang Yuanqing, Wang Zhongxing. *Advances in Materials Science and Engineering*[J], 2016, 2016: 2 941 874
- Zhang Jing, Yang Donghua, Wang Dongya et al. *Journal of University of Science and Technology Beijing*[J], 2008, 30 (12): 1388 (in Chinese)
- Yang Tinghui, Zhang Xinping, Gu Chunfei et al. *The Chinese Journal of Nonferrous Metals*[J], 2010, 20(10): 1890 (in Chinese)
- Ma M, Huo P, Liu W C et al. *Materials Science and Engineering A*[J], 2015, 636: 301
- Jinguo Luo, Acoff Viola L. *Materials Science and Engineering A*[J], 2004, 379(1-2): 164
- Wu K, Chang H, Maawad E et al. *Materials Science and Engineering A*[J], 2010, 527(13-14): 3073
- Zhang X P, Castagne S, Yang T H et al. *Material and Design* [J], 2011, 32(3): 1152
- Zhang X P, Yang T H, Castagne S et al. *Materials Science and Engineering A*[J], 2011, 528(4-5): 1954
- Liu C, Wang Q, Jia Y Z et al. *Materials Science and Engineering A*[J], 2012, 556: 1
- Luo Changzeng, Liang Wei, Chen Zhiqiang et al. *Materials Characterization*[J], 2013, 84: 34
- Nie Huihui, Liang Wei, Chen Hongsheng et al. *Materials Science and Engineering A*[J], 2018, 732: 6
- Luo Changzeng, Liang Wei, Li Xianrong et al. *Material Science Forum*[J], 2013, 747-748: 346
- Lee K S, Lee Y S, Kwon Y N. *Materials Science and Engineering A*[J], 2014, 606: 205
- Kim J S, Lee K S, Kwon Y N et al. *Materials Science and Engineering A*[J], 2015, 628: 1
- Gajanan A, Motagondanahalli R R, Hanumanthappa S N et al. *Journal of Materials Research*[J], 2017, 32(12): 2249
- Wang Taolue, Nie Huihui, Mi Yujie et al. *Journal of Materials Research*[J], 2018, 34(2): 344
- Shen Guanlin, Hu Gengkai, Liu Bin. *Mechanics of Composite Materials*[M]. Beijing: Tsinghua University Press, 2013 (in Chinese)
- Liang Lilin. *Finite Element Simulation of the Hot Roll Bonding Process of TC4-6061 Laminated Composite*[D]. Qinhuangdao: Yanshan University, 2015: 12 (in Chinese)
- Huang Liang. *Simulation and Parameter Analysis of Hot Compounding Rolling of Stainless Clad Plate*[D]. Qinhuangdao: Yanshan University, 2004: 44 (in Chinese)
- Su Guanqiao. *Manufacture and Interface Diffusion of Al/AZ31/Al Layered Composite Plate*[D]. Anshan: University of Sci-

ence and Technology Liaoning, 2015: 21 (in Chinese)  
26 Gong Bao. *Hot Rolling Composite Simulation of NM400/  
Q345R and Its Microstructure Properties and Analysis*[D]. Tai-

yuan: Taiyuan University of Science and Technology, 2018: 31  
(in Chinese)

## 6061 Al/AZ31B Mg/6061 Al对称复合板的组织与力学性能

杨霞<sup>1</sup>, 贺东升<sup>1,2</sup>, 杜晓钟<sup>1</sup>, 王荣军<sup>1</sup>

(1. 太原科技大学机械工程学院, 山西太原 030024)

(2. 晋西工业集团有限责任公司, 山西太原 030024)

**摘要:** 在理论分析与模拟计算的基础上, 通过热轧制备了6061 Al/AZ31B Mg/6061 Al对称复合板, 并对其组织结构和力学性能进行了研究。首先通过经典复合板理论计算得到了复合板中6061 Al的最佳包覆率, 再通过有限元方法模拟得到了复合板的最佳压下率。依据理论分析和仿真计算得到了铝的最佳包覆率和复合板的最佳压下率, 对6061 Al/AZ31B Mg/6061 Al复合板进行组坯, 并在不同轧制温度、不同压下率和不同退火时间下进行了轧制实验, 最后对实验得到的复合板进行了拉伸性能测试、微观组织和能谱分析。结果表明, 在复合板的复合界面处的镁层中发现了再结晶晶粒, 且界面上形成了由 $Mg_{17}Al_{12}$ 和 $Mg_2Al_3$ 组成的金属间化合物; 随着轧制压下率的增大, 6061 Al/AZ31B Mg/6061 Al复合板的抗拉伸强度、延伸率和界面扩散厚度显著增大; 随着轧制温度的升高, 复合板的抗拉伸强度、延伸率和界面扩散厚度也增大; 而随着退火时间的增加, 复合板的抗拉伸强度降低, 但界面扩散厚度增加。

**关键词:** 多层复合材料; 界面结合强度; 层间组织演变; 结合层厚度

---

作者简介: 杨霞, 女, 1981年生, 博士, 副教授, 太原科技大学机械工程学院, 山西太原 030024, 电话: 0351-6998115, E-mail: yangxia@tyust.edu.cn